

A comparison of the combined load behaviour of spudcan and caisson foundations on soft normally consolidated clay

M. J. CASSIDY*, B. W. BYRNE† and M. F. RANDOLPH*

Experimental data from loading tests of model circular footings on soft normally consolidated clay are presented. The experiments were carried out on a drum centrifuge at a radial acceleration level equivalent to 100 times Earth's gravity, ensuring conditions of stress similitude between the model and the prototype scale. The aim of the experiments was to compare the undrained response of different offshore foundations to the same loading conditions. Two different types of foundation were targeted for investigation: spudcans and suction caissons. The spudcan, typically an inverted shallow cone, is the traditional footing for mobile drilling units (also known as jack-up rigs). An alternative foundation concept that is being increasingly considered is that of foundations skirted about the perimeter and installed by suction. A loading arm that incorporated an internal hinge was used so that combinations of load appropriate to the foundations of jack-up units could be applied to the models. Although it was anticipated that, by using skirted foundations there would be increased moment capacity, this was not found to be the case (for the caisson skirt length and soil strength profile investigated). However, there was a stiffer response and additional horizontal capacity at the foundation level. Significantly the use of skirted foundations allowed for a greater combined loading capacity under tensile vertical loads. The results have been interpreted within the framework of strain-hardening plasticity theory, and comparisons with existing yield surfaces are detailed.

KEYWORDS: footings/foundations; centrifuge modelling; offshore engineering; bearing capacity; plasticity; clays

Nous présentons les données expérimentales provenant d'essais de chargement sur des assises circulaires modélisées dans une argile tendre normalement consolidée. Les expériences ont été faites sur un tambour centrifuge avec un niveau d'accélération radiale équivalant à 100 fois la gravité terrestre, assurant des conditions de similitude de contrainte entre l'échelle du modèle et celle du prototype. Le but de ces expériences était de comparer la réponse non drainée des différentes fondations offshore aux mêmes conditions de chargement. Deux types de fondations différentes ont été ciblés pour cette investigation : les spudcans et les caissons à succion. Le spudcan, qui est un cône creux inversé, est l'assise traditionnelle pour les unités de forage mobiles (connues aussi sous le nom de plateformes autoélévatrices). Un autre concept de fondation est de plus en plus considéré ; c'est celui de fondations à jupe sur le pourtour et installées par succion. Un bras de chargement qui contenait une charnière interne a été utilisé de façon à ce que des combinaisons de charge appropriées aux fondations d'unités autoélévatrices puissent être appliquées aux modèles. Nous avions prévu que, en utilisant les fondations jupées, il y aurait une capacité de moment accrue, mais cela n'a pas été le cas (pour la longueur de la jupe du caisson et le profil de résistance du sol étudiés). Cependant, il y a eu une réponse plus rigide et une capacité horizontale additionnelle au niveau de la fondation. De manière significative, l'utilisation de fondations à jupe a permis une capacité de charge combinée plus grande sous charges de traction verticales. Nous avons interprété les résultats dans le cadre de travail de la théorie de plasticité à durcissement par l'effort et nous donnons le détail des comparaisons avec les surfaces d'écoulement existantes.

INTRODUCTION

Engineers are often required to evaluate the behaviour of shallow foundations subject to inclined and eccentric loads (i.e. horizontal loads, H , and moments, M , in addition to central vertical loads, V). This is especially true in the offshore industry, where, during a storm, environmental wind and wave forces impose significant horizontal loads and overturning moments on offshore foundations, as well as alter the vertical load. One example is the foundations of jack-up rigs—mobile drilling units that perform the majority of the world's offshore drilling, in water depths up to 120 m. Most rigs use circular inverted conical footings known as *spudcans* as their foundations, and there is considerable interest within the offshore industry in determining the amount of moment restraint they provide. Further, as the rigs are increasingly being considered for permanent deployment

and in harsher conditions, alternative foundation solutions that provide greater reliability are being considered.

One alternative is suction-installed skirted foundations, commonly known as *suction caissons*. A suction caisson is essentially an 'upturned bucket': that is, a flat circular footing with skirting around the perimeter. The suction caisson is forced into the seabed by developing a net positive pressure across the top of the foundation by withdrawing the water from within the caisson compartment (i.e. 'sucking' it into the ground). It has been thought that the skirt of the caisson may allow for a greater moment and horizontal capacity than provided by a flat footing, such as a spudcan. However, to date there has been no study devoted to comparing the response of the different foundations when subjected to the same loading conditions. The experiments described in this paper therefore aim to:

- compare the response of spudcan and caisson foundations to combined loading conditions on normally consolidated clay. Importantly, they will be compared at loading ratios relevant to mobile drilling rigs.
- provide sufficient experimental information to assess the validity of existing numerical studies. Particular emphasis will be placed on the shape of yield and

Manuscript received 24 January 2003; revised manuscript accepted 3 September 2003.

Discussion on this paper closes on 1 September 2004, for further details see p. ii.

* Centre for Offshore Foundation Systems, University of Western Australia.

† Department of Engineering Science, University of Oxford, UK.

failure surfaces that have been derived and which could be used in plasticity models of the foundations.

Although the main motivation for this study was to compare the response of shallow foundation options for jack-up units, it was possible to investigate loading conditions that might be applicable to other topical offshore applications. One example is the proposed use of caissons for offshore wind turbines, the structures of which might be about 100 m high with rotor diameters of 100 m (Houlsby & Byrne, 2000; Byrne & Houlsby, 2002).

EXPERIMENTAL EQUIPMENT

Experimental geotechnical drum centrifuge

The experimental programme was carried out on the drum centrifuge at the University of Western Australia (Stewart *et al.*, 1998). The soil sample is contained in the 1.2 m diameter outer channel, which is 300 mm high (vertically) and has a 200 mm radial depth. By using two concentrically driven shafts, relative motion between the outer channel, containing the soil sample, and a central tool table can be achieved and controlled. The tool table can therefore be stopped to allow instrumented testing tools to be modified or changed without affecting the acceleration level on the soil. Located on the tool table is a set of actuators that provide both vertical and radial motion relative to the outer channel. These, combined with a specially devised loading leg, allow a combination of vertical, horizontal and rotational motion to be applied to the model foundations.

The primary advantage of using the drum centrifuge for the testing of shallow foundations is the large plan area of the test sample, approximately 300 mm wide by 1440 mm long. The sample depth was approximately 140 mm. All tests were performed at 100g, so the model dimensions corresponded to a prototype testing area 30 m by 144.5 m and 14 m deep. This allowed a considerable number of test sites with consistent soil characteristics to be exploited.

The various scaling relationships for modelling at enhanced accelerations are shown in Table 1, and all results in this paper are presented in terms of equivalent prototype units (though in the figures the scaling relationships used to derive the values have also been shown). In most cases the derived pressure have also been reported.

Loading apparatus

Both in the structural analysis of offshore structures and when considering the combined loading of foundations, a simplification from three-dimensional to planar loading is often made. The loads on a single footing consist of vertical (V), moment (M) and horizontal (H) loads applied in plane. These loads, as well as their corresponding displacements, are shown in Fig. 1, following the sign convention recommended by Butterfield *et al.* (1997). In order to describe the

Table 1. Centrifuge scaling relationships

Quantity	Relationship (model/prototype)
Gravity	N
Stress	1
Strain	1
Length	$1/N$
Force	$1/N^2$
Moment	$1/N^3$
Density	$1/N^2$
Mass	$1/N^3$
Time (consolidation)	$1/N^2$

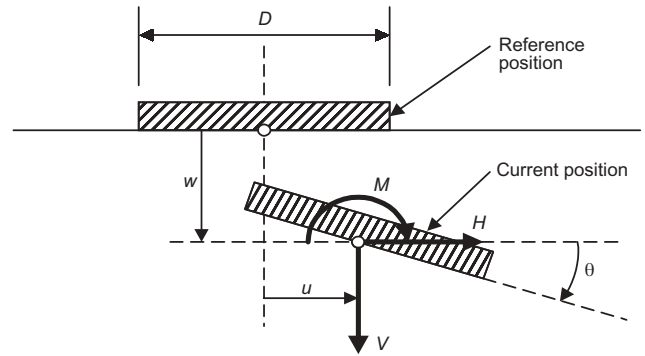


Fig. 1. Sign convention adopted (after Butterfield *et al.*, 1997)

results in this paper in a dimensionally consistent manner and forming work conjugate pairs, the loads are presented as ($V, M/D, H$) and the displacements as ($w, D\theta, u$), where D is the footing diameter.

Typically, in centrifuge modelling, combined loads are applied by translating a stiff loading leg connected to the foundation (Tan, 1990; Dean *et al.*, 1993; Watson & Randolph, 1997, 1998). However, this applies significantly more horizontal load relative to moment than is usually encountered by the foundations of offshore structures. This is definitely the case for jack-up rigs, where typical moment to horizontal load ratios at the foundations could be expected to be in the region of $M/DH \approx 2.5$ (Cassidy *et al.*, 2001; Vlahos *et al.*, 2001). To achieve a ratio similar to this, for the centrifuge tests discussed here, a hinge was placed within the loading leg, as shown in Fig. 2. This allows direct rotation of the foundation about its load reference point, as opposed to the fixed arm test, which can only apply a horizontal displacement (with practically no rotation). Consequently, the use of the hinge allows a much more realistic load ratio to be imposed in the experiment.

The loading leg designed for this experimental programme is shown in Fig. 3. It can be attached easily to the main loading actuator on the centrifuge tool table. The radial and vertical motions of the centrifuge actuator allow any combination of vertical and horizontal load to be applied to the top of the loading arm. Translation through a hinged joint allows a rotation to be applied to the footing, with the ratio of horizontal to moment load fixed by the length of the lever arm. The loading arm can be assembled with or without the hinged joint, so that translational (fixed arm) as well as rotational tests (hinged arm) can be performed. As the purpose of this series of tests was to make comparisons between similar foundations, the footing diameter was kept constant at 60 mm (prototype 6 m). The spudcan and caisson attachments used are shown in Fig. 4, and the whole

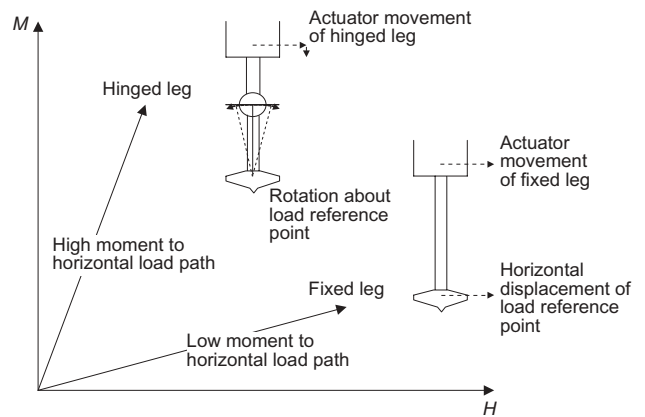


Fig. 2. Expected load paths in moment–horizontal load space for the hinged and fixed legs

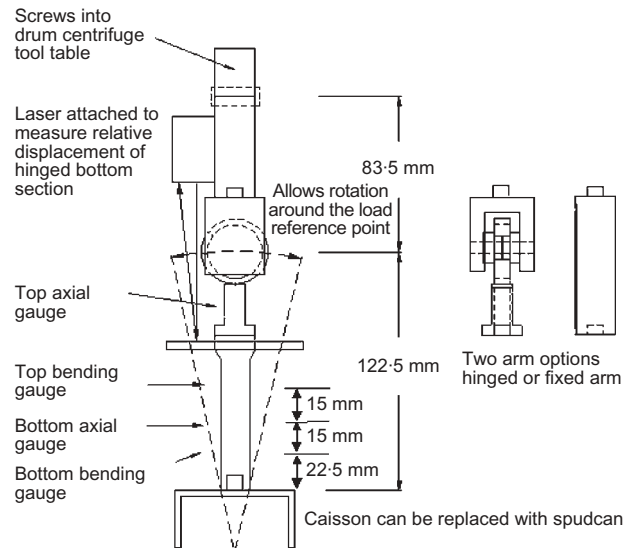


Fig. 3. Design of loading leg used in the experiments

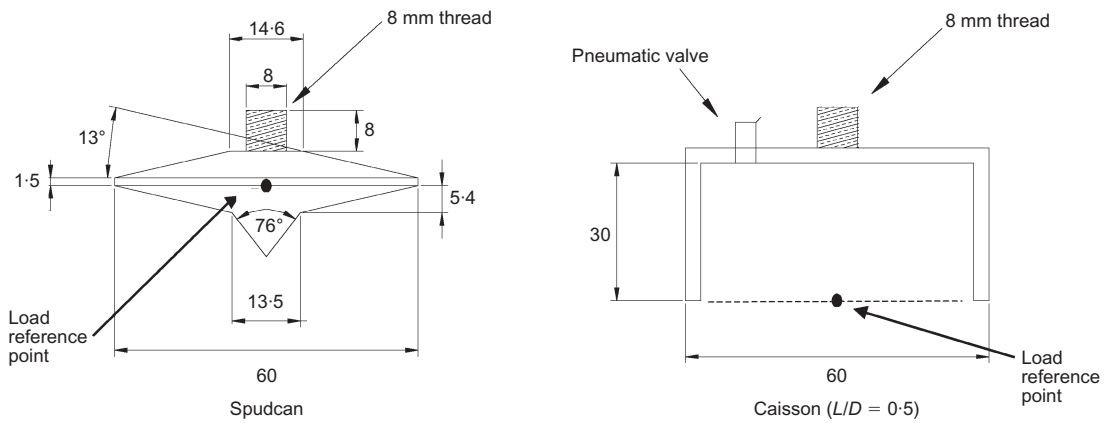


Fig. 4. Model spudcan and caisson footings used in experiments (all dimensions in mm)

apparatus is shown in the photographs in Fig. 5. The skirt length to diameter ratio of the caisson (L/D) was 0.5.

Measuring footing loads and displacements

The load and displacement reference points for the spudcan and caisson are shown in Fig. 4. For the spudcan the load and displacement reference point is the first point of

maximum diameter, assuming the spudcan is penetrating into the soil. For the caisson it has been assumed at the base of the skirts, as this is the most convenient location for comparing the results with those of the spudcan. In reality, considering structural analyses, the load and displacement reference point would be taken at the centre of the underside of the caisson base plate, as this is reflective of where the caisson connects to the structure.

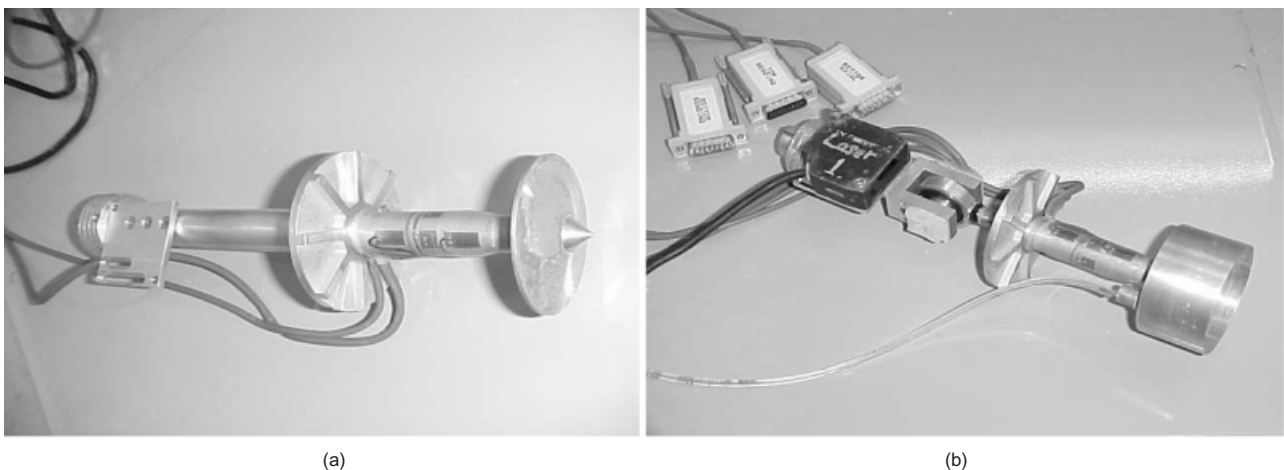


Fig. 5. The loading arms: (a) fixed arm with spudcan; (b) hinged arm with caisson ($L/D = 0.5$)

Shown in Fig. 3 are the strain gauge locations used to determine the loads applied to the foundations. The bending moments determined from the two sets of bending gauges were used to deduce the shear force. In turn, this shear force was used to calculate the moment at the footing's load reference point. Displacement of the footing was measured through a combination of the actuator's vertical and radial movements and a laser located on the loading arm (described in detail in Cassidy & Byrne, 2001). The components of the measured axial and shear forces were also resolved, based on the rotation, so that the true vertical and horizontal loads acting on the footing could be determined (see Fig. 1).

Caisson installation

In an offshore installation caissons could either be sealed after installation or be vented throughout their operation life. With the main application of these experiments being for jack-up on long-term deployment the former installation procedure was of most interest. For this case, the caisson would usually be installed by 'sucking' the water out of the internal cavity. This drives the skirts into the seabed. However, this method was not possible in these experiments, so the caisson skirts were driven into the ground using the radial actuator. A specially designed pneumatic valve (Watson, 1999) was attached to the caisson that allowed fluid to escape from the internal cavity during the installation process. Once the caisson base plate had made contact with the soil surface, as deduced by a stiffer load-displacement response, and therefore representing a fully installed caisson, the valve was closed by applying a pressure of 400 kPa via an airline. The caisson was sealed during the loading experiments.

SOIL CONDITIONS

The soil used throughout the testing programme was a saturated kaolin clay with the key properties given in Table 2 (after Stewart, 1992). The samples were prepared by mixing the kaolin powder with water under vacuum and then pumping the mixed slurry into the channel of the drum (above a 15 mm thick sand layer) while spinning at an acceleration level of 20g. Specific details of the soil preparation and placement method are presented in Cassidy & Byrne (2001). The resulting sample was approximately 140 mm deep (14 m in prototype scale) with a normally consolidated profile. Throughout the entirety of the testing the water table was kept above the surface of the soil sample.

Soil characterisation tests were performed using a T-bar penetrometer at a rate of 1 mm/s (Stewart & Randolph, 1991, 1994; Watson, 1999). The non-dimensional velocity vD/c_v (where v is the velocity, D the appropriate length dimension and c_v the coefficient of consolidation) was above 30, ensuring that undrained behaviour was obtained (Finnie,

1993). One T-bar test was performed next to and on the same day as every footing test to attain an estimate of the shear strength profile. All of the T-bar test results are shown in Fig. 6. They show a strength profile that could be idealised as linearly increasing with a strength gradient of 1.1 kPa/m. However, there is also a slight concavity, and a linear profile would overestimate the shear strength at shallower penetration depths (the depths of the combined loading tests are shown in Fig. 6). Further, the experiments were performed over 9 days, and there was a slight variation of the strength profile over that period. Therefore, for all of the data presented in this paper, the shear strength was assumed to be the average of the two T-bar tests performed directly either side of the combined loading test. These shear strength values, along with the values assuming a 1.1 kPa/m linear increase with depth, are given for the penetration of the swipes in Tables 3 and 4.

INTERPRETATION OF THE EXPERIMENTS

Strain hardening plasticity theory

Experiments are most usefully conducted and interpreted within the context of an appropriate theoretical model. For the combined loading of shallow foundations there are many advantages in casting the problem within the framework of strain hardening plasticity theory. This idea was first used by Roscoe & Schofield (1956) as a geotechnical solution to analyse the foundations of steel frames. However, only recently has a concerted effort by other researchers led to more widespread modelling success for shallow foundations. The advantage of adopting a strain hardening plasticity framework is that the non-linear behaviour of soils can be accommodated within a consistent theoretical framework. With the response of the foundation expressed purely in terms of force resultants on the footing, and with the removal of the ad hoc factors used in traditional bearing capacity, the plasticity framework allows the foundation model to be directly inserted into a numerical analysis of a structure as a 'macro-element'. Some examples of the successful implementation of plasticity models with the structural analysis of jack-ups can be found in, among others, Schotman (1989), Martin (1994), Williams *et al.* (1998), Martin & Houlsby (1999) and Cassidy *et al.* (2001, 2002b).

For analysing spudcan footings within structural analyses, current state-of-the-art strain hardening plasticity models include:

- (a) *Model B*. Based on a series of Ig experiments on overconsolidated clay, Model B is a strain hardening

Table 2. Kaolin clay properties (after Stewart, 1992)

Property	Value
Liquid limit, LL: %	61
Plastic limit, PL: %	27
Plasticity index, I_P : %	34
Specific gravity, G_s	2.60
Angle of internal friction, ϕ'	23°
Consolidation coefficient (mean), c_v : m ² /year	2
Submerged unit weight, γ' : kN/m ³	6.82

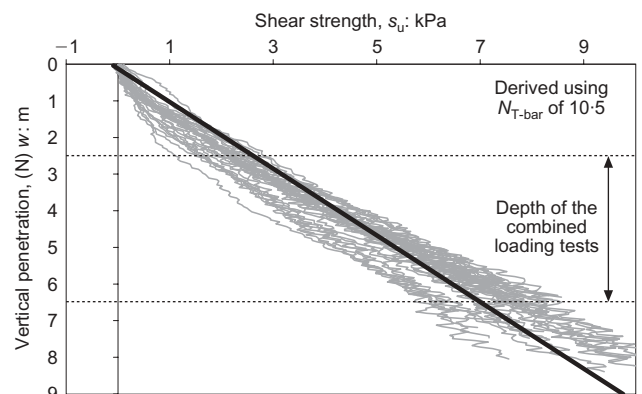


Fig. 6. Strength profiles determined for each of the 32 test sites

Table 3. Details of swipe tests presented

Test name*	Arm	Swipe number	V : MN	V_0 : MN	w : m	s_u using 1·1z: kPa	s_u T-bar either side: kPa	Ref. name (Cassidy & Byrne, 2001)	Figure
S1	Hinged	1	0·842	0·842	2·97	3·27	2·4	BBMCT204	Figs 8(a), 9, 10
		2	1·153	1·153	3·98	4·38	3·4		
		3	1·436	1·436	4·94	5·43	4·4		
S2	Hinged	1	−0·026	0·830	2·81	3·09	2·6	BBMCT213	Fig. 11
S3	Hinged	1	−0·197	0·850	2·69	2·96	3·1	BBMCT215	Fig. 11
S4	Fixed	1	0·912	0·912	3·02	3·32	3·3	BBMCT208	Fig. 16
		2	1·285	1·285	4·01	4·41	4·7		
		3	1·578	1·578	4·97	5·47	5·9		
C1	Hinged	1	0·576	1·000	3·01	3·31	2·6	BBMCT206	Figs 8(b), 17, 18
		2	1·268	1·268	3·96	4·36	3·8		
		3	1·877	1·877	5·99	6·59	6·7		
C2	Fixed	1	0·594	0·992	3·38	3·72	2·7	BBMCT207	Figs 19, 20
		2	0·922	0·922	3·52	3·87	2·8		
		3	1·268	1·268	4·30	4·73	3·8		
		4	1·601	1·601	5·50	6·05	5·7		
		5	1·919	1·919	6·02	6·62	6·5		
		6	2·352	2·352	6·95	7·65	7·4		

*S, spudcan; C, caisson.

V , V_0 and w represent values at the beginning of the swipe.

plasticity model describing the load–displacement behaviour of spudcan footings on clay (Martin, 1994; Martin & Houlsby, 2000, 2001).

- (b) *Model C*. This model is based on a series of 1g experiments on dry dense silica sand (Gottardi *et al.*, 1999; Houlsby and Cassidy, 2002), and is similar in principle to Model B. Model C has been extended so that it is capable of also modelling footing response on dry loose uncemented carbonate sand (Cassidy *et al.*, 2002a).

The major components necessary to develop a strain hardening plasticity model for the combined loading of shallow foundations are:

- an empirical expression for the *yield surface* in combined loading space
- a *strain hardening expression* to define the variation of vertical load with vertical displacement. Most experimental studies have shown that the yield surface of shallow foundations expands and contracts with vertical plastic penetration and plastic heave respectively. They have also shown that, whereas the yield surface size is determined by the vertical load capacity (or maximum vertical load experienced by the footing for the spudcan), the shape remains relatively constant. This is a basic assumption of Model B (Martin, 1994; Martin & Houlsby, 2000, 2001). However, it has also been observed as a useful idealisation by Gottardi *et al.* (1999) for flat footings on drained dense sand, by Watson (1999) and Byrne (2000) for caissons on sand, and by Zhang (2001) for partially embedded pipelines on calcareous sands.
- a suitable *flow rule* to allow predictions of the footing displacements during yield
- a model for *elastic* load–displacement behaviour within the yield surface.

These components can be determined from a combination of experimental investigation, theoretical approaches and numerical studies.

The yield surface shape is the focus of the comparison between the spudcan and caisson foundations given in this

paper. Existing surfaces that are of importance to this study include:

- the yield surface of Model B: determined by experimental observation of 125 mm diameter spudcans on heavily overconsolidated clay (Martin, 1994; Martin & Houlsby, 2000, 2001)
- suggested failure envelopes for flat and caisson foundations from the theoretical and numerical finite element studies of Bransby & Randolph (1998) and Taiebat & Carter (2000). These failure surfaces could be used within plasticity macro-models by assuming associated flow and using theoretical bearing capacity approaches for the strain hardening expression.

Swipe tests

To examine the shape of the yield surface the combined loading ‘swipe’ test was used. In this test the footing is penetrated into the ground to a particular vertical load, at which point the footing is driven horizontally and/or rotated while the vertical penetration is kept constant. Tan (1990), Martin (1994) and Martin & Houlsby (2000) have argued that the load path followed during the test is a close approximation to the yield surface appropriate to that vertical penetration. The caveat is that the ratio of the vertical elastic stiffness to the vertical plastic stiffness must be large (see Martin & Houlsby, 2000, for a thorough explanation of the theoretical rationale behind the test), or a correction must be applied (such as by Gottardi *et al.*, 1999). A number of investigations have used this technique successfully, including:

- conical and spudcan footings on saturated sand (Tan, 1990)
- spudcan footings on overconsolidated clay (Martin, 1994)
- flat footings on dense sand (Gottardi *et al.*, 1999)
- flat footings on carbonate sand (Byrne & Houlsby, 2001)
- caissons in dry dense sand (Byrne & Houlsby, 1999)
- caissons in carbonate sand (Watson, 1999)

Table 4. Additional swipe information for Figs 21 and 22

Test name*	Arm	Swipe number	V : MN	V_0 : MN	w : m	s_u using 1-lz: kPa	s_u T-bar either side: kPa	Ref. name (Cassidy & Byrne, 2001)	Figure
S2	Hinged	2	-0.014	1.128	3.77	4.15	3.9	BBMCT213	Figs 21, 22
		3	0.057	1.479	5.19	5.71	6.0		
S3	Hinged	2	-0.253	1.043	3.25	3.58	3.8	BBMCT215	
		3	-0.281	1.337	4.36	4.80	5.2		
S5	Fixed	1	0.687	0.922	2.80	3.08	3.0	BBMCT209	
		2	1.451	1.451	4.48	4.93	5.4		
		3	0.565	1.845	5.91	6.50	7.2		
S6	Fixed	1	0.169	0.949	2.89	3.18	2.8	BBMCT212	
		2	0.156	1.324	3.93	4.32	4.2		
		3	0.158	1.697	5.36	5.90	6.6		
S7	Fixed	1	0.305	1.029	3.20	3.52	3.1	BBMCT217	
		2	-0.184	1.182	3.53	3.88	3.5		
		3	-0.406	1.436	3.93	4.32	4.0		
S8	Fixed	1	-0.295	0.995	2.56	2.82	2.1	BBMCT232	
		2	1.219	1.219	3.58	3.94	3.4		
		3	1.452	1.452	4.28	4.71	4.4		
C3	Hinged	1	0.147	1.590	3.00	3.30	2.7	BBMCT214	
C4	Hinged	1	-0.267	1.020	2.92	3.21	3.0	BBMCT216	
C5	Hinged	1	-0.379	1.000	2.98	3.28	2.6	BBMCT226	
C6	Hinged	1	-0.325	0.910	3.08	3.39	2.7	BBMCT227	
C7	Hinged	1	-0.890	0.950	2.96	3.22	2.8	BBMCT228	
C8	Fixed	1	0.586	1.038	3.07	3.38	3.2	BBMCT210	
		2	0.683	1.363	4.35	4.79	4.8		
		3	0.948	1.788	5.41	4.95	6.3		
C9	Fixed	1	0.016	0.310	3.13	3.45	3.0	BBMCT211	
		2	0.072	1.116	3.63	4.00	3.8		
		3	0.122	1.499	4.78	5.26	5.4		
C10	Fixed	1	-0.259	1.198	3.13	3.44	3.2	BBMCT218	
		2	-0.227	1.467	4.24	4.67	4.5		
		3	-0.216	1.610	4.65	5.11	5.1		
C11	Fixed	1	-1.038	0.980	2.95	3.24	3.0	BBMCT230	
		2	1.020	1.020	3.49	3.84	3.6		
C12	Fixed	1	-1.079	1.0036	2.96	3.26	2.7	BBMCT231	
		2	0.996	0.996	3.48	3.76	3.4		
		3	1.522	1.522	4.74	5.22	5.1		

*S, spudcan; C, caisson.

V , V_0 and w represent values at the beginning of the swipe.

(g) pipelines on carbonate sand (Zhang, 2001).

Numerical analysis of shallow foundations has confirmed close proximity of swipe paths in (V, H) and (V, M) space to the 'failure' envelope, with agreement between probe tests of fixed displacement ratio and swipe tests (Bransby & Randolph, 1998; Gourvenec & Randolph, 2003).

Figure 7 illustrates the typical swipe-test load paths. Swipe 1 shows a swipe directly after the footing has been penetrated to a vertical load of V_0 (defining the maximum vertical load previously experienced by the footing). Swipes 2 and 3 are investigating the yield surface at low vertical load levels (the footing first being loaded to V_0). In swipe 2 elastic behaviour is assumed until the yield surface is reached. Different regions of the yield surface can be tracked in this way, including investigation of the tensile loading region. To develop the full three-dimensional nature of the yield surface it is necessary to probe the surface at different ratios of moment and horizontal load.

A key part of the swipe test is to ensure that the vertical displacement remains constant so that vertical plastic penetration and therefore hardening of the yield surface during the test is minimised. In the fixed arm experiments the vertical movement can be locked so that no vertical displacement occurs. In the hinged arm experiments the tests

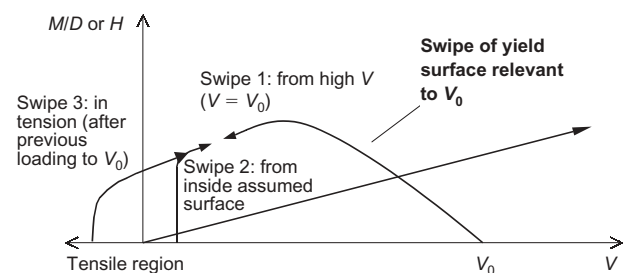


Fig. 7. Expected load paths for the experimental plasticity tests

performed were 'pure' rotation swipes carried out by rotating the hinge in a circular arc about the load reference point (as shown in Fig. 2). During the test small vertical and horizontal movements occur, as the soil-structure system is not infinitely stiff. However, as the ratio of vertical stiffness is about 100:1, the small vertical displacements do not lead to any significant hardening of the yield surface during the test. The 'pseudo-swipe' using the hinged leg would therefore track a close approximation to the yield surface.

Normalisation of yield surfaces (and swipe test results at different vertical penetrations)

The yield surface can either be normalised by V_0 , the bearing capacity under pure vertical load (as suggested by Martin & Houlsby, 2001, for Model B) or by As_u , where A is the plan area of the foundation and s_u is the shear strength at the current depth of the load reference point. This latter approach to normalisation is usually favoured by numerical modellers, but also proves necessary when considering the caisson foundation. Within this paper both normalisations are performed to allow comparisons of the experimental results with the yield surface of Model B (by V_0) and the failure surface of Taiebat & Carter (2000) (by As_u). To compare the spudcan with the caisson, As_u has been used to normalise the results. Further details of the normalisation procedures are given when the experimental results are described.

EXPERIMENTAL RESULTS

There were 32 individual footing tests performed on the one drum centrifuge sample, although only selected results are presented in this paper. Details of these, including test name, vertical load and penetration at the start of each swipe, V_0 and the shear strength assumed, are presented in Tables 3 and 4. Table 3 is for results presented in Figs 8–20 and Table 4 has the additional data shown only in the normalised plots of Figs 21 and 22. The full collection of experimental results can be found in Cassidy & Byrne (2001).

Vertical loading

A typical vertical loading test of a spudcan on soft clay is shown in Fig. 8(a) (test S1). The load–penetration curve displays a very low plastic stiffness that increases slightly with penetration owing to the increase in strength with depth of the clay. The typical loading rate was 1 mm/s, which, using the correlations of Finnie (1993), was chosen to ensure that the tests were undrained. During all spudcan tests collapse of the resulting soil wall and backflow over the back of the spudcan occurred. This occurred by clay flowing around the footing almost immediately after the spudcan’s full diameter (at the load reference point) penetrated into the

ground. During this particular test (test S1) three swipe tests were also performed, as shown by the three significant reductions in load at constant vertical penetrations of approximately 3.0 m, 4.0 m and 5.0 m. After the loading test was completed the footing was extracted from the soil. Fig. 8(a) shows that significant tension capacity was developed and that there is a reduction in vertical stiffness as the footing crosses the zero load line. The backflow material above the spudcan impedes any direct drainage path to the underside of the caisson, and suction are therefore present. During pull-out the clay is assumed to be flowing around the spudcan (very little soil was left on top of the spudcan after it was withdrawn), with the tensile capacity lowered owing to the reduced shear strength of the remoulded soil (Byrne & Cassidy, 2002). A 70% reduction in undrained shear strength was also reported for the tensile pull-out of repeated T-bar tests by Watson (1999). If the spudcan was subjected to a lasting tensile load these suctions could not be sustained and a lower tensile capacity would be observed.

In Fig. 8(b) a typical vertical loading test for a caisson is shown. In contrast with the spudcan response there is little penetration resistance while the skirts are penetrating the soil until the base plate makes contact with the seabed. On making contact (and after the installation valve is closed) there is a sharp increase in the load until a bearing capacity failure occurs. At this stage the footing penetrates plastically into the ground with a similar stiffness to the spudcan footing. In Figs 8(a) and (b) the other footing’s response curve is shown in shadow for comparison. Further discussion about the vertical load response of the foundations, including bearing capacity factors derived from the experiments, can be found in Byrne & Cassidy (2002). In test C1 one swipe was conducted prior to the bearing capacity failure and another two after the caisson had been penetrated below the soil surface.

With the different vertical load responses highlighted in Fig. 8 more consideration of an appropriate normalising procedure can be discussed. It can be seen in Fig. 8(a) that the spudcan undergoes a bearing capacity failure as soon as it starts penetrating into the soil. It is continuously deforming the soil plastically. Therefore the normalisation by V_0 , the maximum vertical load previously experienced by the footing, is valid (as V_0 is a function of As_u the latter would also be valid). However, the caisson is slightly different as

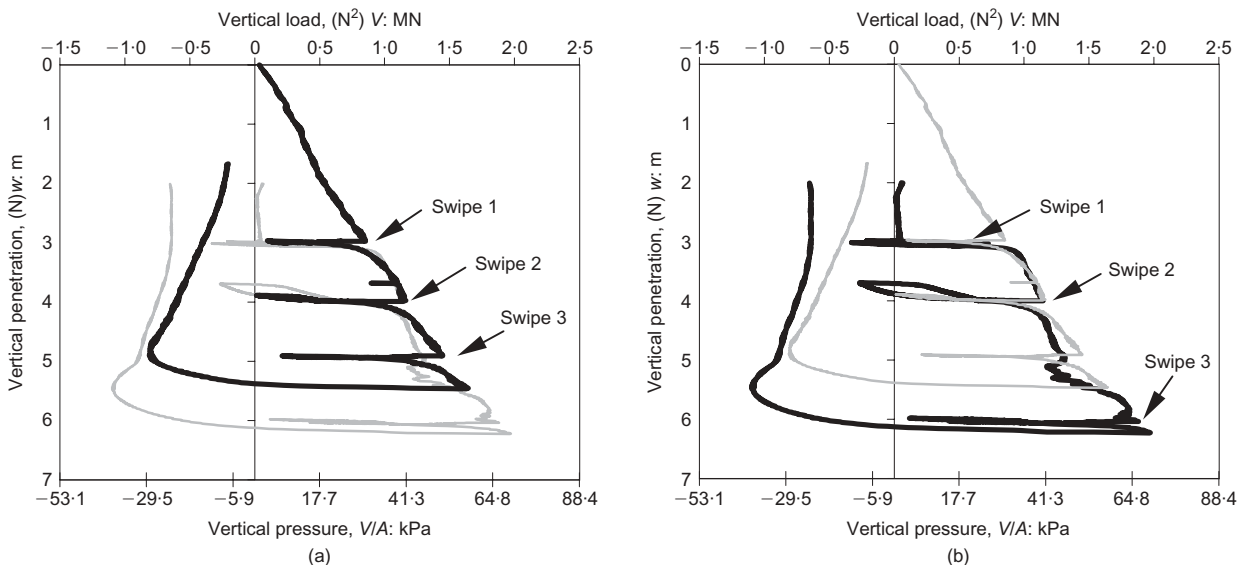


Fig. 8. Vertical load–displacement paths for: (a) a spudcan (S1); (b) a caisson (C1)

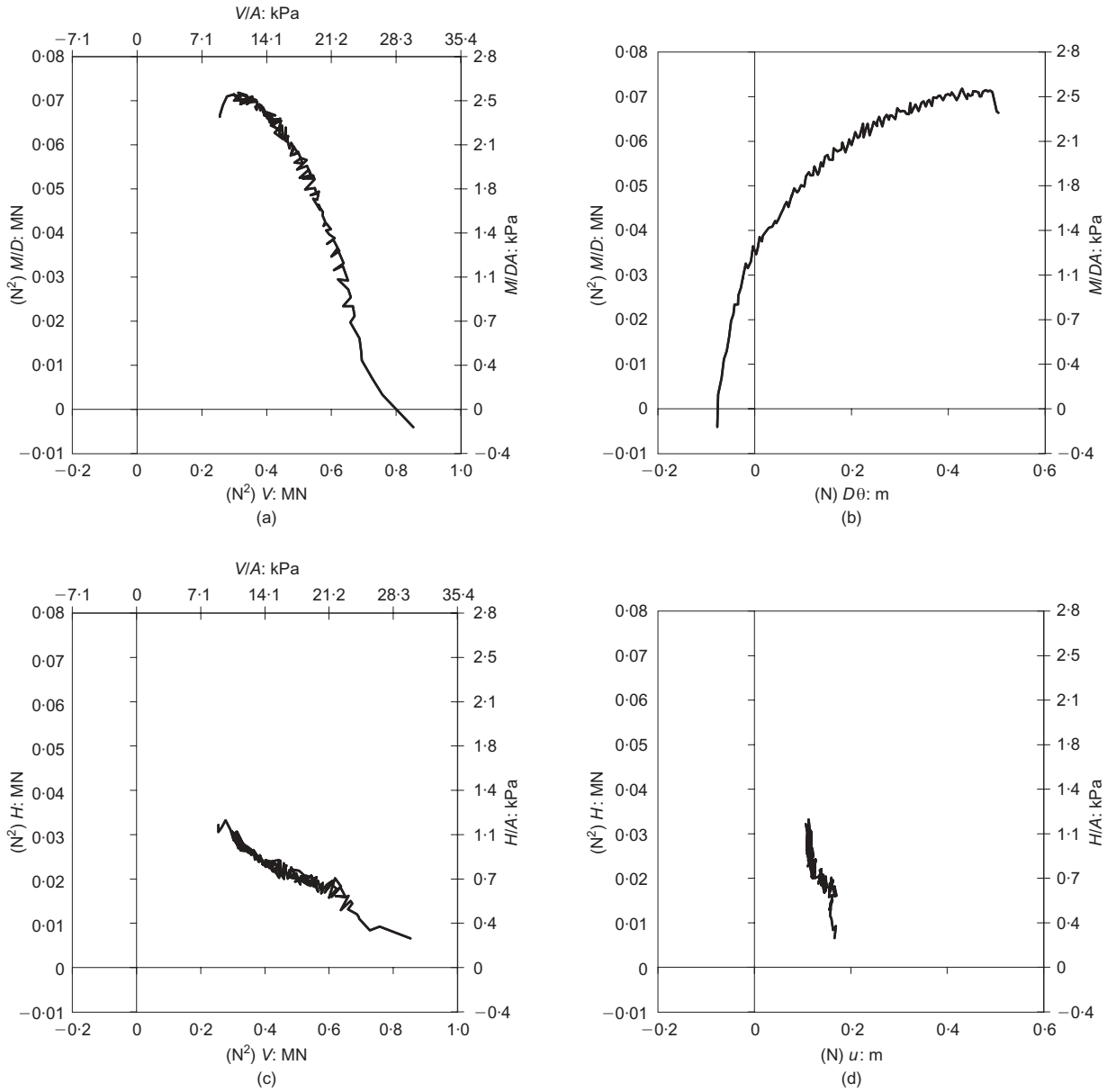


Fig. 9. Initial swipe test for a spudcan using the hinged loading arm (S1)

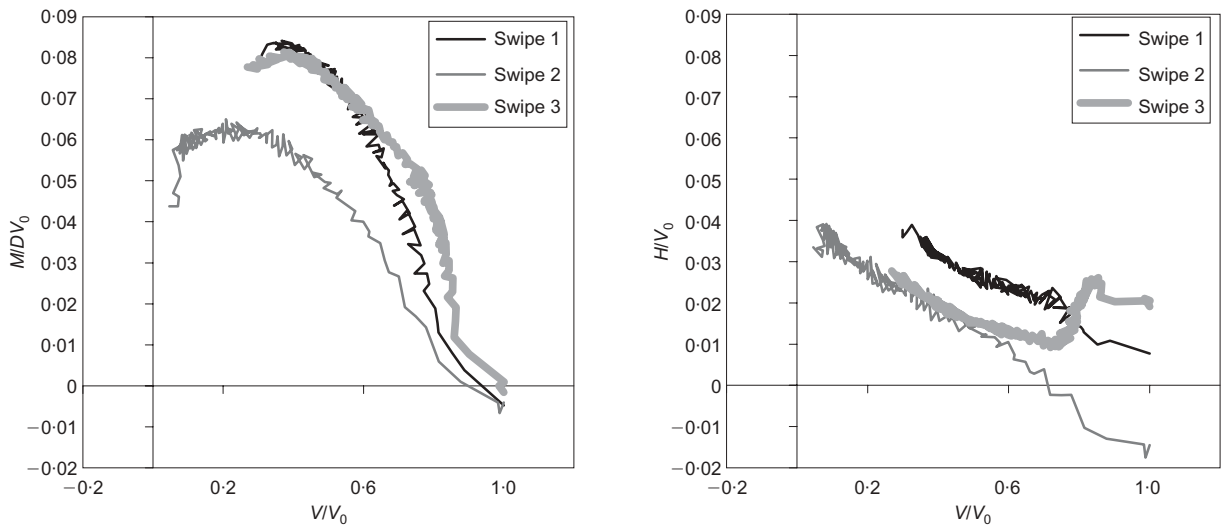


Fig. 10. Normalised load paths for test S1

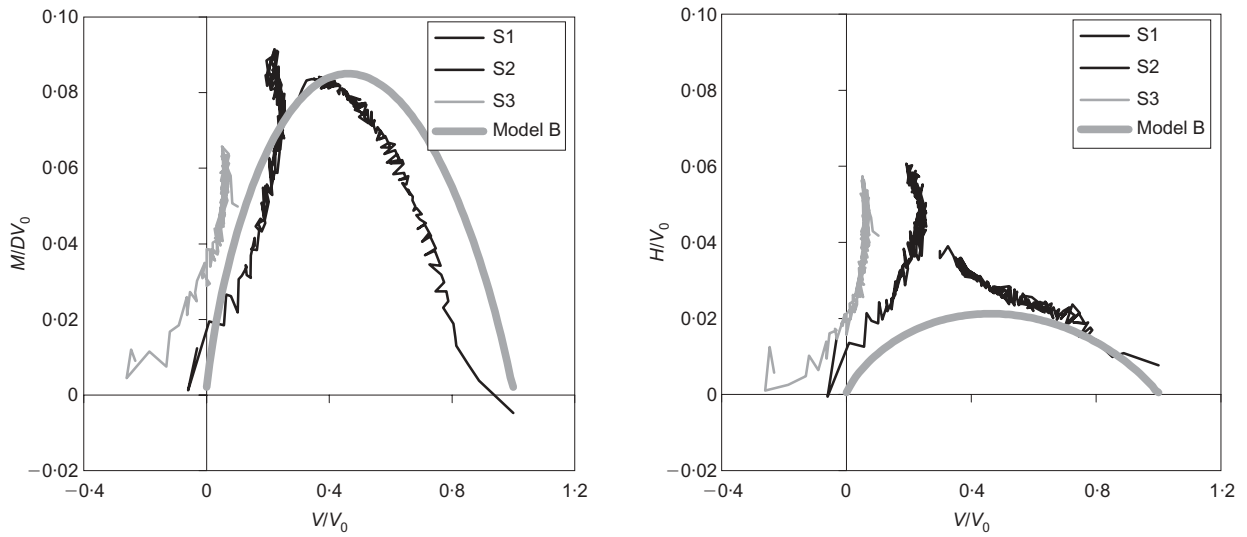


Fig. 11. Normalised swipe tests compared with yield surface of Model B (Martin, 1994; Martin & Houlsby, 2001)

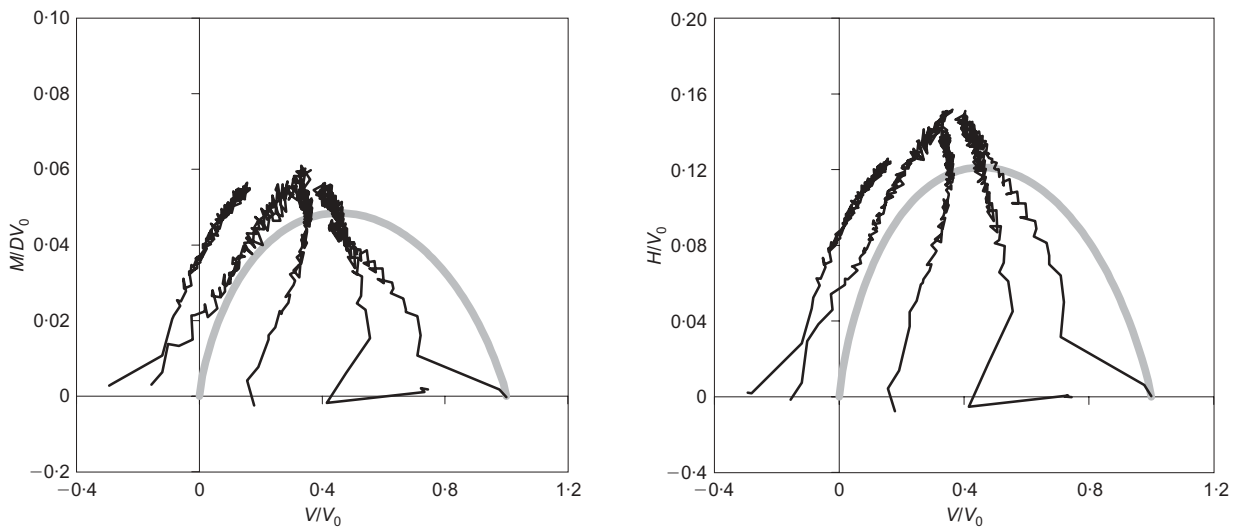


Fig. 12. Normalised fixed arm swipe tests compared with yield surface of Model B

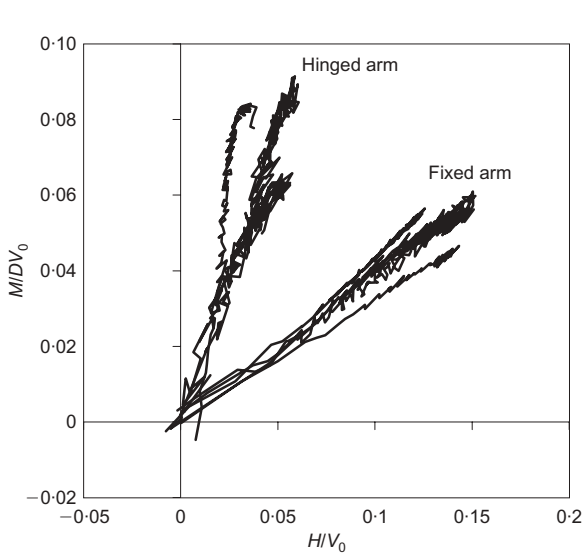


Fig. 13. Results in moment-horizantal load space

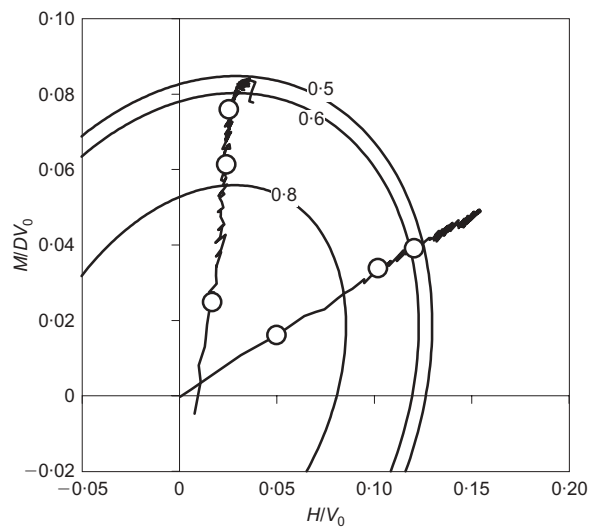


Fig. 14. Comparison with the yield surface of Model B: markers and elliptic curves at $V/V_0 = 0.8, 0.6$ and 0.5

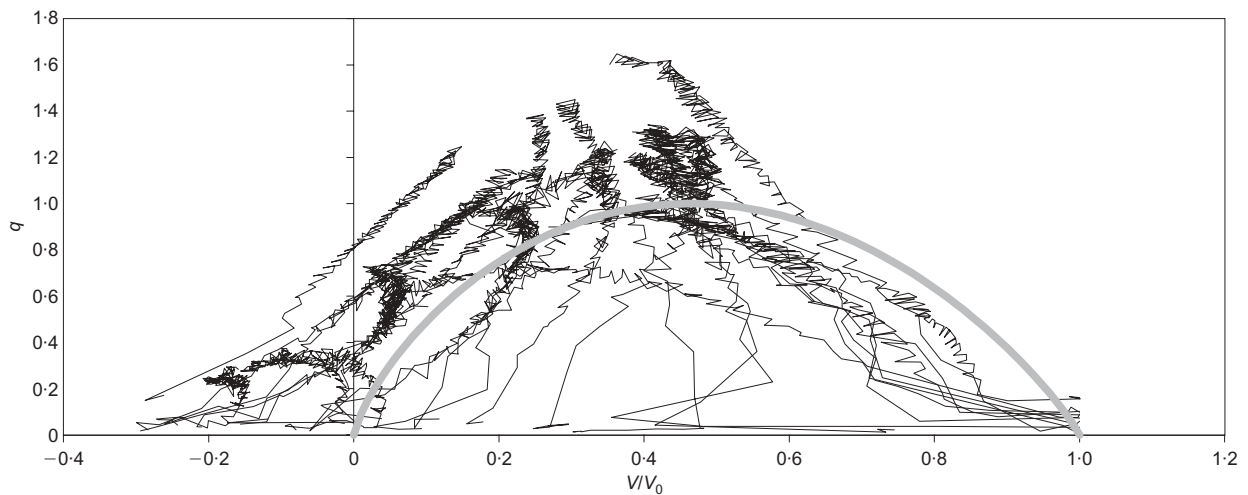


Fig. 15. All spudcan swipe tests in a normalised space compared with the yield surface of Model B

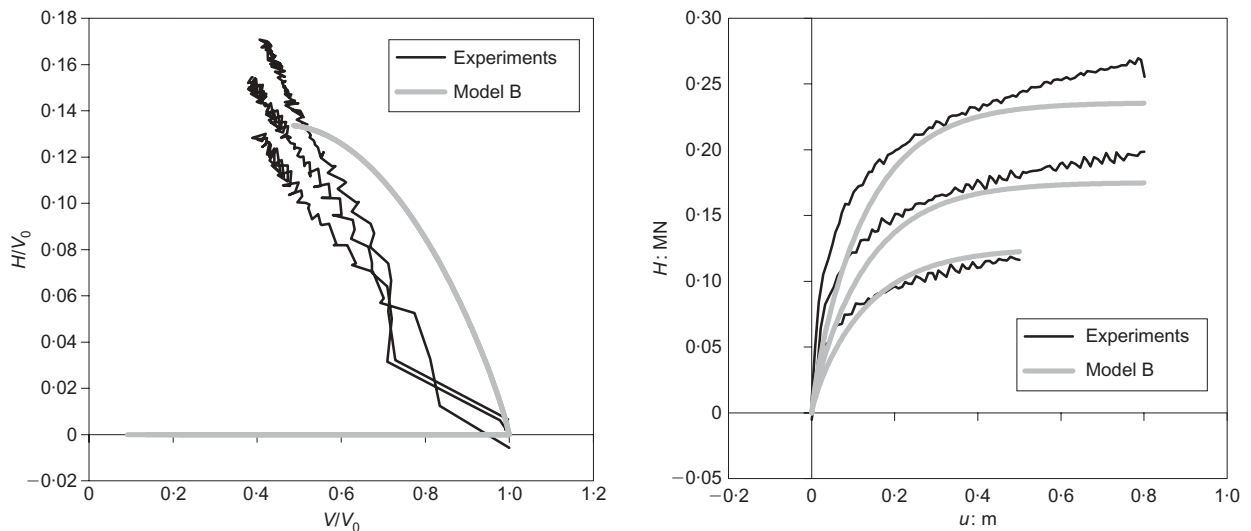


Fig. 16. Model B simulation of the fixed arm swipe test S4

the skirts transfer the failure mechanism much deeper within the soil strata. On loading of the caisson there is a rapid increase in load as the caisson base plate bears on the soil surface. The load increases until a bearing capacity failure occurs. At this point the stiffness reduces dramatically and the footing responds similarly to the spudcan to any further increases or decreases in load. It is clear that, until the initial bearing capacity failure occurs for the caisson, it is inappropriate to normalise by the maximum load previously applied to the footing. It is more appropriate to normalise by the full bearing capacity (including the base plate) or by A_{s_u} . For the latter the shear strength is taken at the base of the caisson skirts and in the case of the spudcan at the level of the maximum diameter (i.e. the load reference point in each case).

Investigation of the yield surface for spudcan footings using the hinged leg

Figures 9(a) and (c) show the load path followed during the swipe phase of the first swipe within test S1, when the

hinged footing was rotated around the load reference point with the vertical displacement held constant. This swipe was performed after the footing had penetrated 2.97 m into the clay, and at this stage the vertical load applied to the foundation was 0.84 MN, as shown in Fig. 8(a). During the swipes, as the moment and horizontal loads increase (and then slightly decrease towards the end of the test), the vertical load continuously decreases. The moment and horizontal load–displacement curve for the same swipe test is shown in Figs. 9(b) and (d).

In all of the footing tests, after each swipe, the spudcan was rotated back to the vertical position and then penetrated further into the ground. During the testing it was assumed that plastically penetrating the footing further into the soil erased the memory of the preceding events. This allowed further swipe tests to be performed on the same site, and therefore a large amount of information could be obtained in a minimum of tests. For site S1 two further swipes were performed at vertical loads depicted in Fig. 8(a) and described in Table 3. In order to compare results the loads are normalised by V_0 , which is the bearing capacity under pure

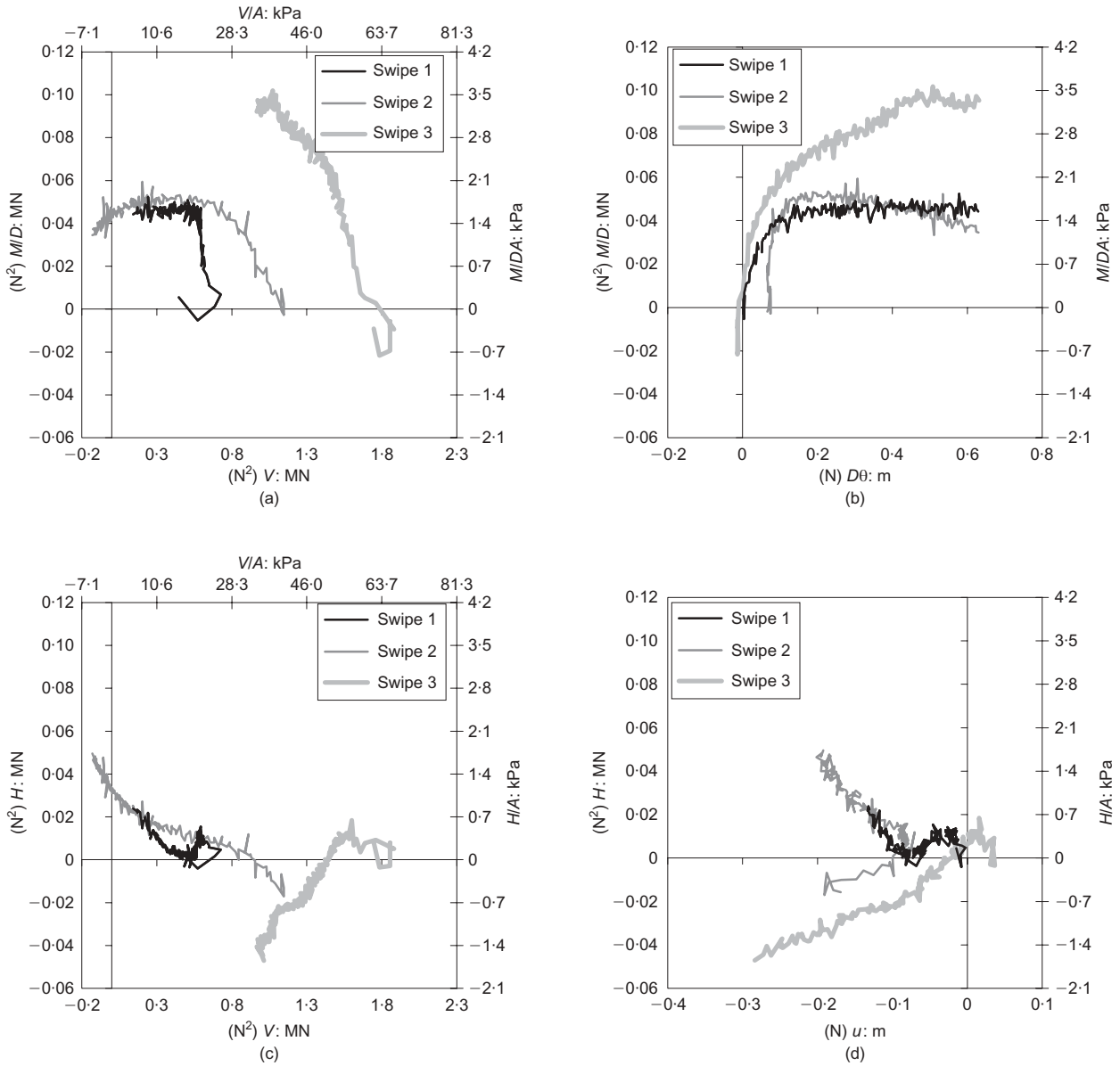


Fig. 17. Swipe tests for a caisson using the hinged loading arm (C1)

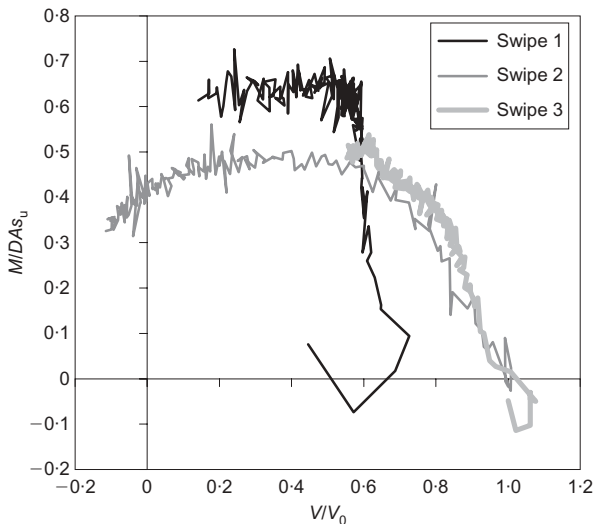


Fig. 18. Normalised swipes for test C1

vertical load, and for the spudcan it is the maximum value of the compressive load previously experienced by the footing. Fig. 10 shows the results of all three swipes normalised in this way. Test S1 represented swipes from the apex of the yield surface ($V/V_0 = 1$).

Two further sets of spudcan swipe tests were carried out using the hinged loading leg. However, these were targeted at exploring the yield surface at low vertical loads. In both tests the foundation was initially loaded to the same vertical load as test S1 (≈ 0.84 MN) and then unloaded to approximately zero vertical load ($V/V_0 \approx 0$) in test S2 and into the tensile region at $V \approx -0.2$ MN ($V/V_0 \approx -0.25$) in test S3. The spudcans were then rotated in a similar manner to test S1. Fig. 11 shows the load paths followed, as well as the results of the swipe from $V/V_0 = 1$ (S1).

Comparison with an existing yield surface

For spudcans on overconsolidated kaolin clay Martin (1994) and Martin & Houlsby (2000, 2001) proposed the

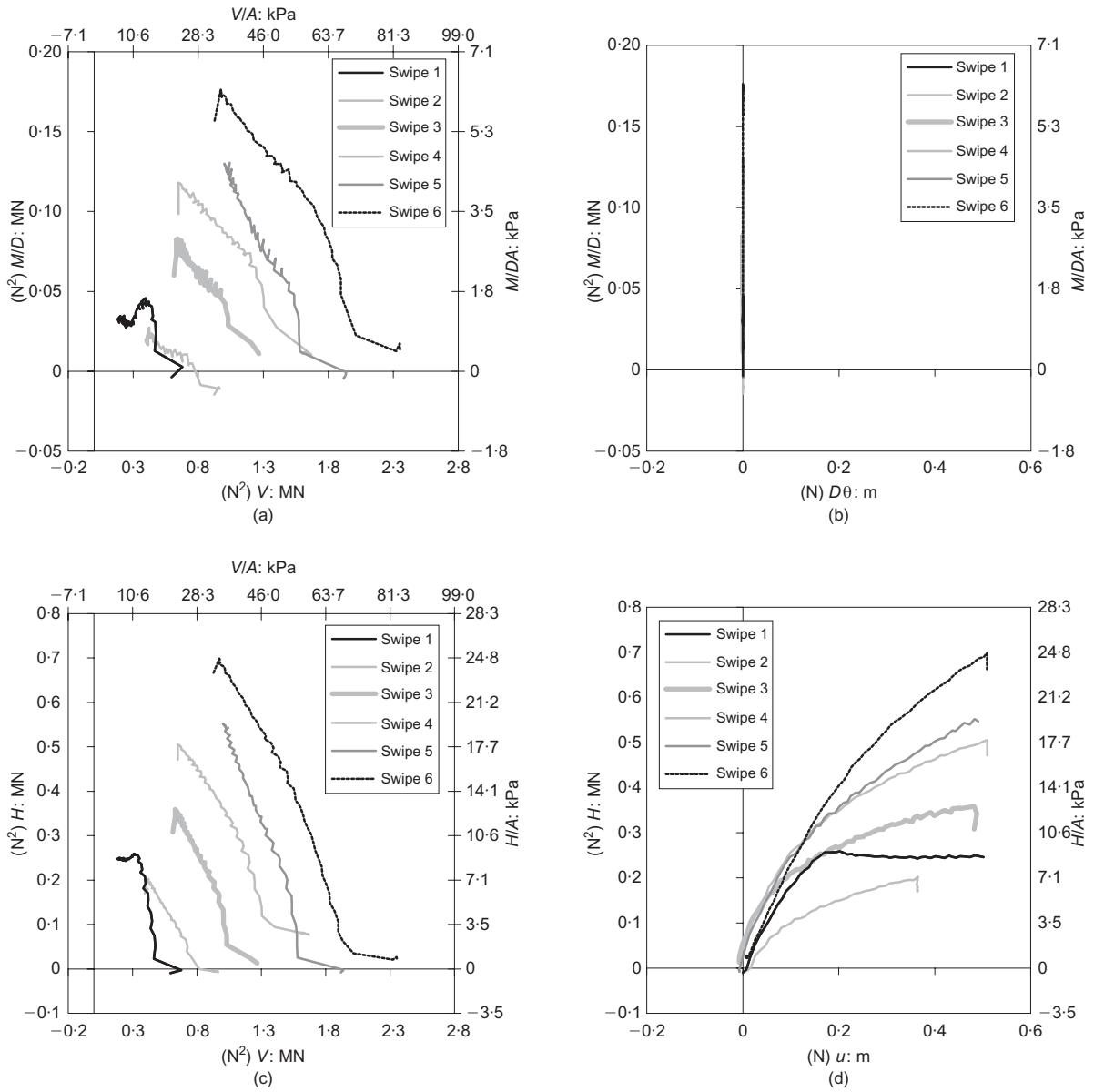


Fig. 19. Swipe tests for a caisson footing using the fixed loading arm (C2)

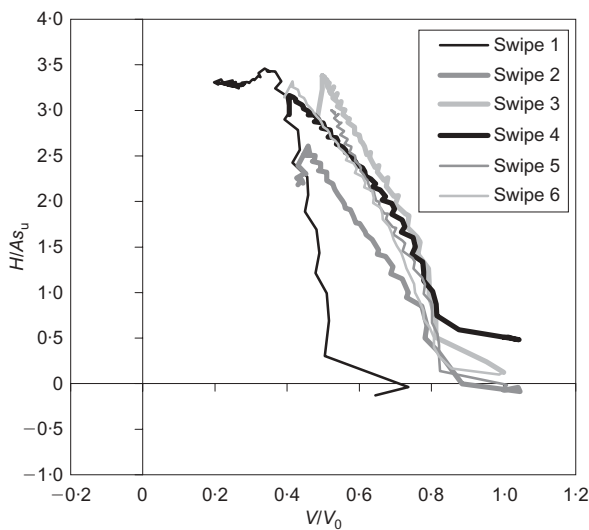


Fig. 20. Normalised swipes for test C2

following empirical equation for the yield surface (for Model B):

$$\left(\frac{M}{M_0}\right)^2 + \left(\frac{H}{H_0}\right)^2 - 2\bar{e}\left(\frac{M}{M_0}\right)\left(\frac{H}{H_0}\right) - \bar{\beta}^2\left(\frac{V}{V_0}\right)^{2\beta_1}\left(1 - \frac{V}{V_0}\right)^{2\beta_2} = 0 \quad (1)$$

where

$$M_0 = m_0 DV_0$$

$$H_0 = h_0 V_0$$

$$\bar{e} = e_1 + e_2\left(\frac{V}{V_0}\right)\left(\frac{V}{V_0} - 1\right)$$

and

$$\bar{\beta} = \frac{(\beta_1 + \beta_2)^{(\beta_1 + \beta_2)}}{\beta_1^{\beta_1} \beta_2^{\beta_2}}$$

V_0 retains the definition previously used: that is, the bearing

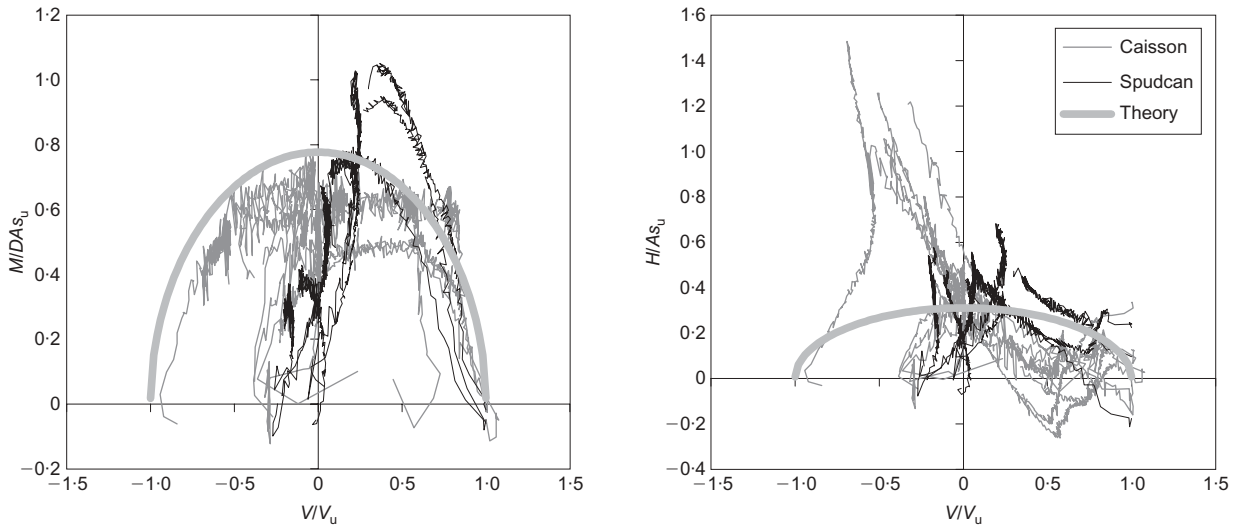


Fig. 21. Comparison of all hinged loading arm data presented in Tables 3 and 4 and scaled surface of Taiebat & Carter (2000)

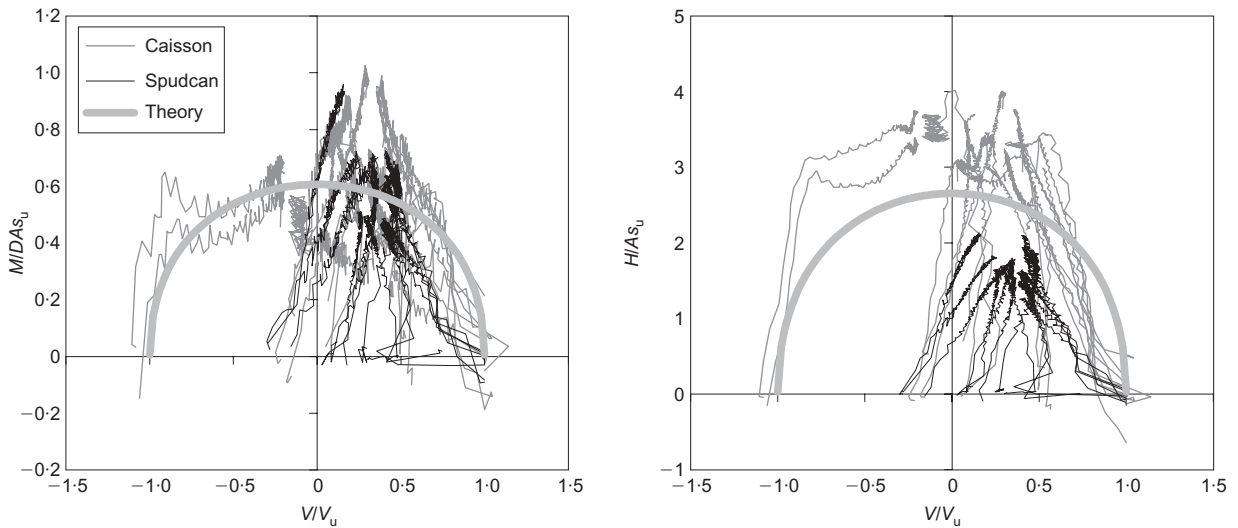


Fig. 22. Comparison of all fixed loading arm data presented in Tables 3 and 4 and scaled surface of Taiebat & Carter (2000)

capacity under pure vertical load. The six parameter values that Martin & Houlsby obtained from regression analysis of their experimental data are: $m_0 = 0.083$, $h_0 = 0.127$, $e_1 = 0.518$, $e_2 = 1.180$, $\beta_1 = 0.764$ and $\beta_2 = 0.882$.

Although equation (1) represents a three-dimensional surface it is possible to plot the representative two-dimensional slice, at the appropriate ratio of M/DH , as shown in Fig. 11. When compared with the experimental results in Fig. 11 the surface shows a reasonable approximation to the data. There is also the indication that a tensile region of the yield surface might be sustained.

Investigation of the yield surface for spudcan footings using the fixed leg

Figure 12 shows swipe tests from various V/V_0 ratios for spudcans loaded with the fixed arm (all of the tests are the first swipe performed at the site). More horizontal load has been applied than for the hinged leg tests shown in Fig. 11. For this slice of the yield surface Model B slightly under-

estimates the capacity at high V/V_0 values but is conservative at low and medium values of V/V_0 . Note that the test procedure adopted by Martin (1994) included a load holding phase prior to the commencement of the swipe test to reduce any creep-related effects. This was not the case in the tests reported here, the swipe being carried out immediately upon reaching the specified vertical penetration. This may have consequences for the shape of the surface, particularly at high vertical loads. It is clear from the reported results that a tension could be sustained and that there is a significant horizontal capacity at zero vertical load.

Discussion of Model B's yield surface

Equation (1) was based on 1g experiments, during which minimal backflow occurred as the footing penetrated into the soil (Martin, 1994; Martin & Houlsby, 2000). An observation during Martin's experiments was that the pure horizontal capacity reduced to zero as the vertical load approached zero (such as would be expected in a drained soil), and this is

represented in equation (1). The experiments reported in this paper show that it might be possible to assume some horizontal capacity at zero vertical load and even negative vertical loads (Figs 11 and 12). From theoretical considerations the undrained horizontal capacity at low vertical loads is equal to As_u , significantly greater than that represented in equation (1). Martin & Houlsby (2000) discuss that, because of the probable shallow failure mechanism for this particular combination of loads (and therefore short drainage paths to the failure zone), true undrained conditions may not have been maintained. However, in the experiments reported in this paper, backflow did occur, and it is highly probable that the lengths of the drainage paths are increased owing to the presence of the remoulded backfill material. The increase in horizontal capacity at zero vertical load confirms this. The horizontal resistance due to the bearing on the sides of the spudcan and loading leg as well as the shear resistance on the top of the spudcan also enhance the horizontal capacity.

Comparing hinged and fixed leg results for the spudcan

Figure 13 shows the different ratios of M/DH for all of the test results shown. It can be seen that the hinged arm allows the exploration of $(M/D, H)$ space in a region not possible with a fixed arm. The two tests representing the swipes from the apex of the yield surface (tests S1 and S4) have been replotted in Fig. 14 with the positions of $V/V_0 = 0.8, 0.6$ and 0.5 highlighted by the markers. The Model B yield surfaces at these load levels have also been displayed in Fig. 14, showing broad agreement with the experimental data.

Both the hinged and fixed arm results can be viewed on the same two-dimensional surface by defining the following quantity (Gottardi *et al.*, 1999):

$$q = \sqrt{\left(\frac{M}{M_0}\right)^2 + \left(\frac{H}{H_0}\right)^2} - 2\bar{e}\left(\frac{M}{M_0}\right)\left(\frac{H}{H_0}\right) \quad (2)$$

This can now be plotted against V/V_0 and fixed and hinged arm results compared. This simple manipulation is shown for the experimental data in Fig. 15. The normalised Model B surface is also shown, calculated using:

$$q = \bar{\beta}\left(\frac{V}{V_0}\right)^{\beta_1}\left(1 - \frac{V}{V_0}\right)^{\beta_2} \quad (3)$$

The tests that start within the yield surface (i.e. those starting from $V/V_0 < 1$) exhibit quasi-elastic response prior to hitting the yield surface. It is clear that the yield surface determined by Martin (1994) provides a lower bound to most of the experimental results. This is particularly the case at low vertical loads. The results at high vertical loads are slightly inside the yield surface. This could be rectified by adjusting the parabola weighting parameters β_1 and β_2 to reflect the slight bias. This requires further investigation, and may be a consequence of (a) the different soil strength profiles and (b) the slightly different test procedures used in the two testing programmes. In particular, it would be useful to conduct 'constant-load probe tests' commencing from high vertical loads to investigate the yield surface further at these values.

Retrospective numerical simulations of the experiments

It is possible to use the Model B plasticity model to predict the load–displacement response of the spudcan. This allows for the retrospective simulation of the physical experiments. This is shown in normalised (V, H) load space and for the horizontal load–displacement curves in Fig. 16.

This shows that both the yield surface and the flow rule in Model B are simulating the experimental behaviour very well.

Results from the caisson experiments

Figure 17 shows swipe tests of the caisson using the hinged leg. Fig. 8(b) indicated the vertical load penetration curve and swipe locations. The first swipe location is prior to a bearing capacity failure whereas swipes 2 and 3 are post bearing capacity failure. The results are similar to those obtained for the hinged spudcan footing, including the magnitude of the peak moment load. Interestingly a negative horizontal load was obtained for the third swipe. This is due to the large vertical load when the leg is tilted, which resolves into an overall negative horizontal load, even though a positive load was deduced at the gauges.

To compare the three swipe tests it is necessary to normalise the loads by a measure of the strength of the clay at that depth: that is, $(V/V_0, M/DAs_u, H/As_u)$, where V_0 is the pure vertical load capacity of the caisson for that penetration. Before vertical bearing failure of the base plate has occurred this will be larger than the maximum vertical load previously experienced by the footing (as used in the spudcan). This normalisation procedure was described in the previous section (Interpretation of the experiments), and the values of V_0 and s_u used to normalise each swipe test are given in Table 3. The normalisation is presented in Fig. 18, which shows that the ultimate moment load is bounded by $M/DAs_u = 0.65$. Swipe 1 begins at $V/V_0 < 1$ as it was performed immediately after installation and before bearing failure. Interestingly this pre-bearing capacity swipe has a much steeper load path prior to yielding at a slightly higher level than the post-bearing capacity swipe tests.

Similar responses can be seen in Fig. 19 for the horizontal loading case, where results for a fixed arm test (C2) are presented. Again, the initial swipe has been carried out prior to full bearing capacity failure and therefore the load path is steeper than the swipes performed post bearing capacity failure.

The normalised horizontal and vertical load results are plotted together in Fig. 20. Swipes 1 and 3–6 appear to reach the same final normalised horizontal load, although the initial load paths are slightly different. The second swipe in both tests indicates a slightly lower normalised capacity. This might be due to insufficient penetration between the two sub-tests and therefore a slight effect from the first swipe sub-test. It is clear from Figs 18 and 20 that, for a newly installed caisson, there exists an outer yield surface sized by the vertical bearing capacity of the footing.

A number of swipe tests were also performed from low vertical loads and from tension, in a similar manner to the spudcan footing. Selected swipe tests are normalised and shown in Figs 21 and 22 for both the caisson and the spudcan. The spudcan results are normalised in the same fashion as the caisson so that a comparison can be made. The first observation is that for the hinged case, where there is a realistic ratio of moment to horizontal load, there appears to be little difference in the moment capacities for a spudcan or a caisson in terms of ultimate magnitude. It would appear that the maximum moment load capacity is bounded by $M/DAs_u = 0.65$. The caisson has a larger combined load capacity in tension as the presence of the skirts allows the undrained reverse bearing capacity failure to be mobilised.

In the fixed arm tests there is a significant difference between response for the caisson and the spudcan. The caisson has a significantly larger horizontal capacity than the similar capacities in the moment plane. The presence of

the skirt around the perimeter of the foundation allows passive and active resistances to be mobilised under the action of the horizontal load. Evidence of a substantial horizontal resistance for embedded caissons under tensile vertical loads was also documented by Watson *et al.* (2000).

The caisson curves are compared in Figs 21 and 22 with the yield surface shape of Taiebat & Carter (2000) for the appropriate ratios of M/DH . They give the following expression for the three-dimensional yield surface of a shallow circular footing lying on the surface of homogeneous undrained soil:

$$\left(\frac{V}{V_u}\right)^2 + \left[\left(\frac{M}{M_u}\right)\left(1 - \alpha_1 \frac{HM}{H_u|M|}\right)\right]^2 + \left|\left(\frac{H}{H_u}\right)^3\right| - 1 = 0 \quad (4)$$

where V_u is the ultimate capacity of the footing under purely vertical load. The sizes of the surface under pure horizontal load (H_u) and pure moment load (M_u) have been determined by an upper bound analysis of a caisson with an aspect ratio of $L/D = 0.5$ and assuming a surface roughness value of 0.3. This results in solutions of $H_u/As_u = 2.97$ and $M_u/DAs_u = 0.754$ respectively. The value of α_1 has been taken to be 0.3. Fig. 21, the hinged arm tests, shows that these theoretical results give a slightly non-conservative estimate for the moment capacity compared with the caissons. The fixed arm results shown in Fig. 22 indicate a reasonable fit in $(V, M/D)$ space, but are fairly conservative in (V, H) space.

Interestingly, the upper bound solution for a circular plate at the same depth (of $0.5D$) gives a slightly higher pure moment capacity than the caisson, with a value of $M_u/DAs_u = 0.88$. This may indicate why the caisson moment capacities were not found experimentally to be greater than those of the spudcans.

CONCLUSIONS

The results from a series of tests on model spudcan and caisson footings in normally consolidated soft clay have been presented. The tests were designed to investigate footing behaviour under combined $(V, M/D, H)$ loading, and to provide data that can be used to validate existing as well as develop new plasticity models. The novelty of the testing was to compare the response of skirted and non-skirted foundations and therefore assess whether improvements in performance could be obtained by the addition of a skirt. In order to apply appropriate loading combinations to the model scale footings in a centrifuge, a hinged loading arm was developed. This allowed higher ratios of moment to horizontal load to be applied to the footings than the more conventional fixed arm approach.

The principal conclusions drawn from the tests are as follows:

(a) The experimental data indicated that no significant improvement in moment capacity could be gained by using the skirted foundation under the loading relevant to jack-up units. However, these results should be considered only for caissons of a similar L/D ratio and soil strength profile. Significant increases in the moment stiffness could be obtained if the skirted foundations were designed to operate at a load significantly lower than their pure bearing capacity. The horizontal capacity, in contrast, was significantly increased by using the skirted foundation. Importantly, the tests indicated that the caisson had a significantly larger combined load capacity under tension than the spudcan.

(b) The current strain hardening plasticity models for predicting the performance of spudcan foundations were shown to be adequate if a little conservative. It might be possible to allow for some tensile capacity and a slightly enlarged yield surface if backflow is known to have occurred. This is an area that requires more investigation before any definitive changes to current practice could be recommended. The experimental results reported here show the shape of the yield surface to be slightly different from that of Martin (1994) and Martin & Houlsby (2000). It is possible that this is due partly due to (i) the differences in the soil strength profiles, where Martin's tests were performed on heavily overconsolidated clay whereas the tests reported here were performed on normally consolidated clay, and (ii) the slightly different test procedure, where Martin (1994) used a load holding phase prior to the swipe test, which was not the case for the tests reported here. However, the existing Model B retrospectively simulated the experimental results at a different stress level successfully.

(c) Failure surfaces derived for flat circular footings by numerical methods were shown to adequately model the yield surface of a caisson with the extension achieved by scaling the ultimate moment and ultimate horizontal load using upper-bound solutions for a caisson.

ACKNOWLEDGEMENTS

These experiments could not have been performed without the support of the drum centrifuge technician Mr Bart Thompson. The helpful advice from Mr George Vlahos during the design of the loading leg and the results from his numerical implementation of Model B are gratefully acknowledged.

This work was undertaken with support from Woodside Energy Limited (Po No: 7500011421) and an IREX grant from the Australian Research Council. The second author also acknowledges the support of the Royal Commission for the Exhibition of 1851, the Apgar Prize and Magdalen College, Oxford. The Centre for Offshore Foundation Systems was established and is supported under the Australian Research Council's Research Centres Programme.

NOTATION

A	foundation area
c_v	coefficient of consolidation
D	foundation diameter
e_1, e_2, \bar{e}	yield surface fitting parameters (Model B)
h_0	dimensionless size factor for yield surface (Model B)
H	horizontal load
L	caisson skirt length
m_0	dimensionless size factor for yield surface (Model B)
M	moment
q	general deviator force
s_u	undrained shear strength
u	horizontal displacement
v	velocity of T-bar test
V	vertical load
V_0	dimension of yield surface in V -direction
w	vertical displacement
$\beta_1, \beta_2, \bar{\beta}$	shaping factors for yield surface (Model B)
θ	rotation

Subscripts

u ultimate capacity

REFERENCES

- Bransby, M. F. & Randolph, M. F. (1998). Combined loading of skirted foundations. *Géotechnique* **48**, No. 5, 637–656.
- Butterfield, R., Houlsby, G. T. & Gottardi, G. (1997). Standardised sign conventions and notation for generally loaded foundations. *Géotechnique* **47**, No. 4, 1051–1052.
- Byrne, B. W. (2000). *Investigations of suction caisson foundations on dense sand*. DPhil thesis, Oxford University, UK.
- Byrne, B. W. & Cassidy, M. J. (2002). Investigating the response of offshore foundations in soft clay soils. *Proc. 21st Int. Conf. Offshore Mechanics Arctic Engng, Oslo*, paper OMAE2002-28057.
- Byrne, B. W. & Houlsby, G. T. (1999). Drained behaviour of suction caisson foundations on very dense sand. *Proc. 31st Ann. Offshore Technol. Conf., Houston*, paper 10994.
- Byrne, B. W. & Houlsby, G. T. (2001). Observations of footing behaviour on loose carbonate sands. *Géotechnique* **51**, No. 5, 463–466.
- Byrne, B. W. & Houlsby, G. T. (2002). Investigating novel foundations for offshore wind turbines. *Proc. 21st Int. Conf. Offshore Mechanics Arctic Engng, Oslo*, paper OMAE2002-28423.
- Cassidy, M. J. & Byrne, B. W. (2001). *Drum centrifuge model tests comparing the performance of spudcans and caissons in kaolin clay*, OUEL Report No. 2248/01. Oxford: Department of Engineering Science, University of Oxford.
- Cassidy, M. J., Eatock Taylor, R. & Houlsby, G. T. (2001). Analysis of jack-up units using a constrained new wave methodology. *Appl. Ocean Res.* **23**, 221–234.
- Cassidy, M. J., Byrne, B. W. & Houlsby, G. T. (2002a). Modelling the behaviour of a circular footing under combined loading on loose carbonate sand. *Géotechnique* **52**, No. 10, 705–712.
- Cassidy, M. J., Taylor, P. H., Eatock Taylor, R. & Houlsby, G. T. (2002b). Evaluation of long-term extreme response statistics of jack-up platforms. *Ocean Engng* **29**, No. 13, 1603–1631.
- Dean, E. T. R., James, R. G., Schofield, A. N., Tan, F. S. C. & Tsukamoto, Y. (1993). The bearing capacity of conical footings on sand in relation to the behaviour of spudcan footings of jack-ups. In *Predictive soil mechanics* (eds G. T. Houlsby and A. N. Schofield), pp. 230–253. London: Thomas Telford.
- Finnie, I. M. S. (1993). *Performance of shallow foundations in calcareous soils*. PhD thesis, University of Western Australia, Perth.
- Gottardi, G., Houlsby, G. T. & Butterfield, R. (1999). The plastic response of circular footings on sand under general planar loading. *Géotechnique* **49**, No. 4, 453–470.
- Gourvenec, S. & Randolph, M. F. (2003). Effect of strength non-homogeneity on the shape of failure envelopes for combined loading of strip and circular foundations on clay. *Géotechnique* **53**, No. 6, 575–586.
- Houlsby, G. T. & Byrne, B. W. (2000). Suction caisson foundations for offshore wind turbines and anemometer masts. *J. Wind Engng* **24**, No. 4, 249–255.
- Houlsby, G. T. & Cassidy, M. J. (2002). A plasticity model for the behaviour of footings on sand under combined loading. *Géotechnique* **52**, No. 2, 117–129.
- Martin, C. M. (1994). *Physical and numerical modelling of offshore foundations under combined loads*. DPhil thesis, University of Oxford.
- Martin, C. M. & Houlsby, G. T. (1999). Jackup units on clay: structural analysis with realistic modelling of spudcan behaviour. *Proc. 31st Offshore Technol. Conf., Houston*, paper OTC 10996.
- Martin, C. M. & Houlsby, G. T. (2000). Combined loading of spudcan foundations on clay: laboratory tests. *Géotechnique* **50**, No. 4, 325–338.
- Martin, C. M. & Houlsby, G. T. (2001). Combined loading of spudcan foundations on clay: numerical modelling. *Géotechnique* **51**, No. 8, 687–700.
- Roscoe, K. H. & Schofield, A. N. (1956). The stability of short pier foundations in sand. *Br. Weld. J.*, August, 343–354.
- Schotman, G. J. M. (1989). The effects of displacements on the stability of jack-up spud-can foundations. *Proc. 21st Offshore Technol. Conf., Houston*, OTC 6026 515–524.
- Stewart, D. P. (1992). *Lateral loading of piled bridge abutments due to embankment construction*. PhD thesis, University of Western Australia.
- Stewart, D. P. & Randolph, M. F. (1991). A new site investigation tool for the centrifuge. *Proc. Int. Conf. Centrifuge Modelling: Centrifuge '91, Boulder*, 531–538.
- Stewart, D. P. & Randolph, M. F. (1994). T-Bar penetration testing in soft clay. *J. Geotech. Engng Div., ASCE* **120**, No. 12, 2230–2235.
- Stewart, D. P., Boyle, R. S. & Randolph, M. F. (1998). Experience with a new drum centrifuge. *Proc. Int. Conf. Centrifuge '98, Tokyo* **1**, 35–40.
- Taiebat, H. A. & Carter, J. P. (2000). Numerical studies of the bearing capacity of shallow foundations on cohesive soil subjected to combined loading. *Géotechnique* **50**, No. 4, 409–418.
- Tan, F. S. C. (1990). *Centrifuge and numerical modelling of conical footings on sand*. PhD thesis, University of Cambridge.
- Vlahos, G., Martin, C. M. & Cassidy, M. J. (2001). Experimental investigation of a model jack-up unit. *Proc. 11th Int. Offshore Polar Engng Conf., Stavanger* **1**, 97–105.
- Watson, P. G. (1999). *Performance of skirted foundations for offshore structures*. PhD thesis, University of Western Australia.
- Watson, P. G. & Randolph, M. F. (1997). A yield envelope design approach for caisson foundations in calcareous sediments. *Proc. 8th Int. Conf. Behaviour of Offshore Structures, Delft*, 259–276.
- Watson, P. G. & Randolph, M. F. (1998). Failure envelopes for caisson foundations in calcareous sediments. *Appl. Ocean Res.* **20**, 83–94.
- Watson, P. G., Randolph, M. F. & Bransby, M. F. (2000). Combined lateral and vertical loading of caisson foundations. *Proc. 32nd Offshore Technol. Conf., Houston*, paper OTC 12195.
- Williams, M. S., Thompson, R. S. G. & Houlsby, G. T. (1998). Non-linear dynamic analysis of offshore jack-up units. *Comput. Struct.* **69**, No. 2, 171–180.
- Zhang, J. (2001). *Geotechnical stability of offshore pipelines in calcareous sand*. PhD thesis, University of Western Australia.